

# Ultrafast Scanning of Exchangeable Sites by NMR Spectroscopy\*\*

Xiang Xu, Jae-Seung Lee, and Alexej Jerschow\*

Chemical exchange saturation transfer (CEST) and magnetization transfer (MT) have become widely popular techniques for generating enhanced MRI contrast in vivo and ex vivo.<sup>[1]</sup> To fully characterize these phenomena and to investigate suitable candidates for contrast agents, the polarization of the reporter signal (typically water) is measured as a function of the frequency offset of the saturating radio-frequency (RF) irradiation (Z-spectrum).<sup>[2]</sup> Here, we present an ultrafast method to obtain a Z-spectrum over a large range of frequency offsets from only two signal excitations. This method can be useful for fast screening of imaging phantoms and para- and diamagnetic chemical exchange saturation transfer (CEST) contrast agents under different experimental conditions (e.g. saturation time and power).

CEST offers the prospect of following biomarkers,<sup>[3]</sup> metabolites,<sup>[4]</sup> and enzymes<sup>[5]</sup> as they participate in the metabolism in tissues and in vivo. Many endogenous as well as exogenous molecules have been identified for the generation of contrast that is based on the exchange of protons from the molecular environment to a bulk water pool.

Examples of endogenous contrast include the measurement of the amide proton transfer (APT),<sup>[3]</sup> glycogen (GlyCEST),<sup>[6]</sup> glycosaminoglycan (gagCEST),<sup>[7]</sup> glutamate (GluCEST),<sup>[8]</sup> and glucose (GlucoCEST)<sup>[9]</sup>, which can become important for helping in the diagnosis and follow-up of diseases such as osteoarthritis and stroke.

The field of exogenous CEST agents is dominated by the development of paramagnetic shift agents (paraCEST) with exchangeable proton sites.<sup>[10]</sup> These can, in principle, allow for high-power irradiation because of the large frequency offsets involved. ParaCEST agents have been used for temperature and pH mapping,<sup>[11]</sup> targeting cells,<sup>[12]</sup> and detecting enzyme

activities.<sup>[13]</sup> Diamagnetic CEST (diaCEST) agents, such as polypeptides and reporter genes have also been developed.<sup>[14]</sup> Recently, the use of hyperpolarized gas as CEST biosensors has also been reported.<sup>[15]</sup>

The proposed method acquires full Z-spectra in only two scans, and could also be combined with additional high-throughput approaches based on imaging multiple samples simultaneously,<sup>[16]</sup> as well as with the use of auto-samplers.

The one-shot acquisition of a Z-spectrum presented here is inspired by “ultrafast” NMR spectroscopic methods,<sup>[17]</sup> henceforth called ultrafast Z-spectroscopy (UFZ spectroscopy). Ultrafast NMR methods typically use spatial encoding of indirect evolution times to speed up multi-dimensional NMR experiments. Thus 2D and 3D ultrafast NMR experiments have been demonstrated, and the principle has also been applied to MRI methodology.<sup>[18]</sup> A one-shot method was proposed for the broadband excitation and acquisition of MT effects,<sup>[19]</sup> but was never used in the context of CEST.

The pulse sequence for UFZ is shown in Figure 1a. During the first gradient pulse, a portion of a sample at a distance  $d$  from the center of the gradient feels an additional external field amounting to  $\Delta B_{\text{sat}}(d) = G_{\text{sat}} d$ , which shifts all resonances in this slice by  $\Delta \omega_{\text{sat}}(d) = \gamma G_{\text{sat}} d$ , where  $\gamma$  is the gyromagnetic ratio of a proton and  $G_{\text{sat}}$  is the strength of the gradient pulse. The saturating RF irradiation is held at the zero offset frequency throughout, hence the slice experiences an effective irradiation of resonances at an offset  $-\Delta \omega_{\text{sat}}(d)$ . During acquisition, the gradient  $G_{\text{acq}}$  (which needs not be of the same strength) produces a shift by  $\Delta \omega_{\text{acq}}(d) = \gamma G_{\text{acq}} d$ .

The Fourier-transformed spectrum of the acquired signal is then plotted versus  $\Delta \omega_{\text{acq}}(d)$ , which is related to the

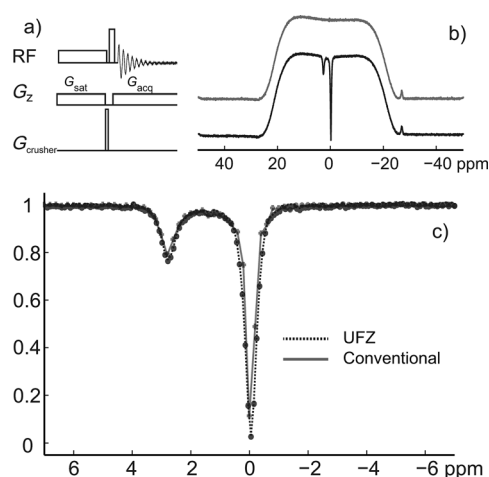


**Figure 1.** a) Pulse sequence for the UFZ spectroscopy. b) Reference spectrum without saturation (upper curve). The raw UFZ spectrum (lower curve). c) A comparison of the conventional Z-spectrum (solid) and the UFZ spectrum (dashed).

[\*] Dr. X. Xu, Dr. J.-S. Lee, Prof. A. Jerschow  
Department of Chemistry, New York University  
100 Washington Sq. East, New York, NY 10003 (USA)  
E-mail: alexej.jerschow@nyu.edu  
Homepage: <http://www.nyu.edu/projects/jerschow/>

Dr. J.-S. Lee  
Center for Biomedical Imaging, Radiology Department  
New York University  
660 First Ave, New York, NY 10016 (USA)

[\*\*] We acknowledge funding from the US National Science Foundation under grant number CHE0957586 (to A. Jerschow) and the National Institutes of Health under grant number K25AR060269 (to J.-S. Lee). X. Xu is grateful for the Margaret and Herman Sokol fellowship. The experiments were performed in the Shared Instrument Facility of the Department of Chemistry, New York University, supported by the US National Science Foundation under grant number CHE0116222. We would like to thank Dr. J. Pekar, Dr. P. C. M. van Zijl, and Dr. M. T. McMahon for helpful discussions.

Supporting information for this article is available on the WWW under <http://dx.doi.org/10.1002/anie.201303255>.

frequency offset of the saturating RF irradiation using  $\Delta\omega_{\text{acq}}(d) = -(G_{\text{acq}}/G_{\text{sat}})\Delta\omega_{\text{sat}}(d)$ . If  $G_{\text{acq}}$  is set to  $-G_{\text{sat}}$ , the frequency reading in the Fourier-transformed spectrum is the same as the frequency offset of the saturating RF irradiation.

By omitting the saturation part before the read pulse, the reference signal at each position can be acquired for normalization. In this way, the UFZ methodology does not require a uniform shape of the sample along the gradient direction as long as the relative concentrations remain constant throughout. The Fourier-transformed spectra obtained from 50 mM glutamic acid in water with and without the saturating RF irradiation are shown in Figure 1b, which produce a normalized Z-spectrum (UFZ spectrum) as seen in Figure 1c.

We demonstrate the UFZ methodology on both diaCEST and paraCEST agents: glutamic acid in water and Eu-DOTA-4AmC (Macrocyclics, 10 mM in  $\text{H}_2\text{O}$ ), respectively. The Z-spectra of 50 mM glutamic acid acquired using both the UFZ and conventional methods are almost identical, as shown in Figure 1c, except that UFZ is 71 times faster (for 71 frequency offsets in this case). The direct saturation appears more symmetric around the resonance frequency of water protons in the UFZ spectrum because of its increased frequency and digital resolution. The ability to precisely determine the minimum of the direct saturation is an appealing trait for MT ratio asymmetry analysis ( $\text{MTR}_{\text{asym}}$ ), in particular when the resonance frequency of exchangeable protons is close to the water resonance.<sup>[20]</sup>

The Z-spectra for different concentrations of glutamic acid acquired with the UFZ method are shown in Figure 2. The  $\text{MTR}_{\text{asym}}$  plots reveal two peaks at 3 and 1 ppm corresponding to the exchangeable amide and hydroxyl protons, respectively. The intensities of both  $\text{MTR}_{\text{asym}}$  peaks become greater with increasing concentration. The slight frequency changes of the peaks are due to pH and relaxation time changes associated with increasing concentrations. The intensity of the  $\text{MTR}_{\text{asym}}$  peak at 3 ppm revealed a linear relationship with the concentration of glutamic acid, except for the higher concentration, as expected.

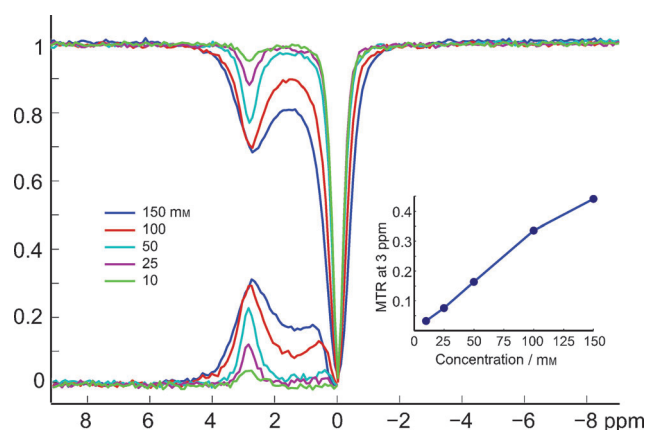


**Figure 2.** UFZ spectra acquired from glutamic acid solutions in water at different concentrations, and the corresponding  $\text{MTR}_{\text{asym}}$  curves. Inset: The intensity of the  $\text{MTR}_{\text{asym}}$  peak at 3 ppm as a function of the concentration.

The speedup of UFZ is also useful when many experiments with varying duration and strength of the saturating RF irradiation need to be performed. For example, Figure 3a and b shows the UFZ spectra of 50 mM glutamic acid with varying saturation duration and power, respectively, acquired within 2 minutes with the UFZ method. This type of analysis is common for estimating parameters such as exchange rates using the QUEST, QUESP, and QUESTRA protocols,<sup>[21]</sup> and for optimizing parameters for CEST contrast and pH measurement.

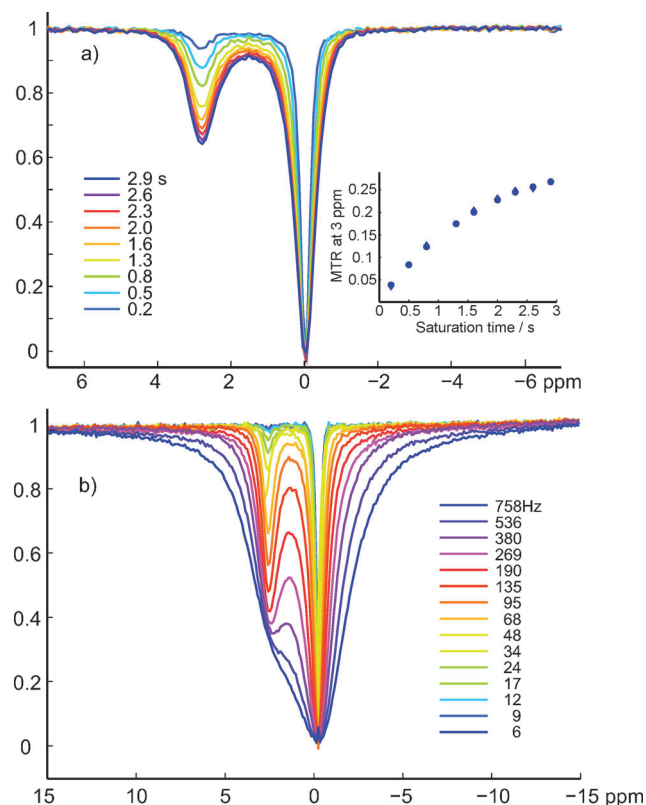


**Figure 3.** The UFZ spectra of 50 mM glutamic acid water solution with varying a) saturation duration and b) saturation power. Inset in (a): The  $\text{MTR}_{\text{asym}}$  at 3 ppm as a function of concentration. At low pH and room temperature, the exchange rate for amine protons analyzed with QUESP and QUEST were 950 and 700 Hz, respectively.

Figure 4 demonstrates the applicability of UFZ to paraCEST. The agent used is Eu-DOTA-4AmC, which has an exchangeable site at 55.6 ppm with respect to the resonance frequency of water protons.<sup>[10]</sup> While the large chemical shifts of the exchangeable sites make paraCEST agents favorable for many applications, it is often tricky to locate the exchangeable sites. Furthermore, the frequency positions can shift strongly in response to environmental effects. Conventional Z-spectra would require time-consuming experiments for localizing the exchangeable sites. In our UFZ method, instead of having the saturation and read-out RF frequency coincide at the water resonance, we shifted the saturation frequency by +30 ppm therefore the direct water saturation appears at -30 ppm. Since the asymmetry analysis is not necessary for paraCEST agents with resonances far

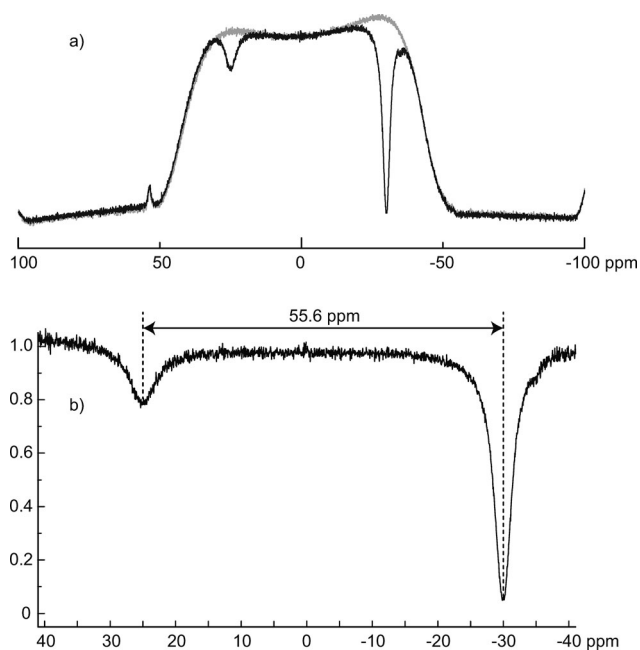


**Figure 4.** UFZ spectra of a 10 mM Eu-DOTA-4AmC water solution. a) The reference (gray) and the raw (black) UFZ spectra. b) The UFZ spectrum: zoomed in between 40 and  $-40$  ppm.

away from water, this scheme allows us to cover a larger frequency range without increasing the gradient strength.

For a quick check of the frequency position of a CEST agent, the normalization may not be necessary, in which case UFZ becomes a single-shot method. On the other hand, the normalization makes the UFZ method robust against the spatial variation in the sample shape or solution distribution, hence the method can be applied over irregular shapes or under severe  $B_0$  inhomogeneity through a sample (see Figure S1 in the Supporting information), as long as the concentration of a CEST agent remains the same. Any additional inhomogeneity would only be reflected in a “squeezing” or stretching of the irradiation frequency axis. A further advantage of UFZ may be that the acquisition of the Z-spectrum in the presence of a gradient would avoid distortions due to radiation damping.<sup>[22]</sup>

Similar to other ultrafast methods, the UFZ method has a lower signal-to-noise ratio (SNR) than the conventional method and limited frequency resolution because of the water diffusion during the saturating RF irradiation. At 25 °C and with a  $3 \text{ G cm}^{-1}$  gradient, for example, water diffusion will lead to broadening of about 90 Hz when the saturation time is 1 s (0.18 ppm at 11.7 T) and the broadening increases linearly as a function of the square root of the saturation time. Diffusion may not affect the UFZ spectrum much if the spread due to diffusion is less than the excitation range of the saturating RF irradiation.

In conclusion, we hope that UFZ can be a helpful tool in the development of new CEST agents or in the systematic study of endogenous CEST mechanisms. The UFZ method can also be useful for the optimization of the so-called uniform-MT method<sup>[23]</sup> and CEST with hyperpolarized gases.<sup>[15]</sup> When optimizing such experiments, one would

have to perform a large number of experiments to find the best parameters, and UFZ would provide a much-needed speedup. The amount of time required to acquire the Z-spectra offers a reliable method to facilitate the rapid screening of many samples, an aspect that could become particularly useful for contrast agent development.

## Experimental Section

All experiments were performed using a Bruker Avance 500 MHz NMR spectrometer equipped with a broadband observe (BBO) probe with triple-axis gradient. All data were acquired at 25 °C.

Five different concentrations (10, 25, 50, 100, and 150 mM) of glutamic acid in water were prepared. The transmitter frequency was set to the resonance frequency of bulk water protons. The duration and strength ( $\gamma B_1/2\pi$ ) of the saturating RF irradiation were 1 s and 48 Hz, respectively. The spectral window was 80 ppm and 1024 data points were acquired. For the conventional Z-spectrum, the frequency offset of the saturating RF irradiation was swept from  $-7$  to  $7$  ppm at a step size of 0.2 ppm, and a  $5^\circ$  read pulse was used to excite the bulk water proton NMR signal. The unwanted residual signal excited by the saturating RF irradiation was removed by a two-step phase cycle of the saturating RF irradiation. The total experiment time was about 35 minutes. For the UFZ method,  $G_{\text{acq}} = -G_{\text{sat}} = 3 \text{ G cm}^{-1}$ , and a  $90^\circ$  read pulse were used. The total experiment time was less than 20 s. Experiments with varying saturation pulse duration (from 0.2 to 2.9 s) and strength (from  $\gamma B_1/2\pi = 6$  to 758 Hz) were performed on the 50 mM solution.

The magnetization transfer ratio,  $\text{MTR}_{\text{asym}}$ , was calculated using  $\text{MTR}_{\text{asym}} = S_{\text{sat}}(\Delta\omega)/S_0 - S_{\text{sat}}(-\Delta\omega)/S_0$ , in which  $S_{\text{sat}}(\Delta\omega)$  is the signal of water with a saturation frequency  $\Delta\omega$  away from the water resonance and  $S_0$  is the water signal without saturation.

For the test with a paraCEST agent, a 10 mM Eu-DOTA-4AmC solution was prepared in pH 7 buffer.  $G_{\text{acq}} = -G_{\text{sat}} = 6 \text{ G cm}^{-1}$ , and the duration and strength of the saturating RF irradiation were 1 s and 1100 Hz, respectively, the frequency of the saturating RF irradiation was shifted by  $+30$  ppm from the reference frequency.

Received: April 17, 2013

Published online: June 28, 2013

**Keywords:** chemical exchange saturation transfer · magnetization transfer · NMR spectroscopy · structure elucidation

- [1] a) S. D. Wolff, R. S. Balaban, *J. Magn. Reson.* **1990**, *86*, 164–169; b) K. M. Ward, A. H. Aletras, R. S. Balaban, *J. Magn. Reson.* **2000**, *143*, 79–87; c) J. Y. Zhou, P. C. M. van Zijl, *Prog. Nucl. Magn. Reson. Spectrosc.* **2006**, *48*, 109–136.
- [2] R. G. Bryant, *Annu. Rev. Biophys. Biomol. Struct.* **1996**, *25*, 29–53.
- [3] J. Zhou, B. Lal, D. A. Wilson, J. Larter, P. C. M. van Zijl, *Magn. Reson. Med.* **2003**, *50*, 1120–1126.
- [4] a) S. Aime, D. Delli Castelli, F. Fedeli, E. Terreno, *J. Am. Chem. Soc.* **2002**, *124*, 9364–9365; b) S. Zhang, R. Trokowski, A. D. Sherry, *J. Am. Chem. Soc.* **2003**, *125*, 15288–15289.
- [5] B. Yoo, M. S. Raam, R. M. Rosenblum, M. D. Pagel, *Contrast Media Mol. Imaging* **2007**, *2*, 189–198.
- [6] P. C. M. van Zijl, C. K. Jones, J. Ren, C. R. Malloy, A. D. Sherry, *Proc. Natl. Acad. Sci. USA* **2007**, *104*, 4359–4364.
- [7] W. Ling, R. R. Regatte, G. Navon, A. Jerschow, *Proc. Natl. Acad. Sci. USA* **2008**, *105*, 2266–2270.
- [8] K. J. Cai, M. Haris, A. Singh, F. Kogan, J. H. Greenberg, H. Hariharan, J. A. Detre, R. Reddy, *Nat. Med.* **2012**, *18*, 302–306.

- [9] K. W. Chan, M. T. McMahon, Y. Kato, G. Liu, J. W. Bulte, Z. M. Bhujwalla, D. Artemov, P. C. M. van Zijl, *Magn. Reson. Med.* **2012**, 68, 1764–1773.
- [10] S. Zhang, M. Merritt, D. E. Woessner, R. E. Lenkinski, A. D. Sherry, *Acc. Chem. Res.* **2003**, 36, 783–790.
- [11] a) S. R. Zhang, C. R. Malloy, A. D. Sherry, *J. Am. Chem. Soc.* **2005**, 127, 17572–17573; b) S. Aime, A. Barge, D. Delli Castelli, F. Fedeli, A. Mortillaro, F. U. Nielsen, E. Terreno, *Magn. Reson. Med.* **2002**, 47, 639–648.
- [12] S. Aime, A. Barge, C. Cabella, S. G. Crich, E. Gianolio, *Curr. Pharm. Biotechnol.* **2004**, 5, 509–518.
- [13] B. Yoo, M. D. Pagel, *J. Am. Chem. Soc.* **2006**, 128, 14032–14033.
- [14] a) M. T. McMahon, A. A. Gilad, M. A. DeLiso, S. M. Cromer Berman, J. W. M. Bulte, P. C. M. van Zijl, *Magn. Reson. Med.* **2008**, 60, 803–812; b) A. A. Gilad, M. T. McMahon, P. Walczak, P. T. Winnard, V. Raman, H. W. M. van Laarhoven, C. M. Skoglund, J. W. M. Bulte, P. C. M. van Zijl, *Nat. Biotechnol.* **2007**, 25, 217–219.
- [15] a) L. Schroder, T. J. Lowery, C. Hilty, D. E. Wemmer, A. Pines, *Science* **2006**, 314, 446–449; b) T. K. Stevens, K. K. Palaniappan, R. M. Ramirez, M. B. Francis, D. E. Wemmer, A. Pines, *Magn. Reson. Med.* **2013**, 69, 1245–1252.
- [16] G. Liu, A. A. Gilad, J. W. M. Bulte, P. C. M. van Zijl, M. T. McMahon, *Contrast Media Mol. Imaging* **2010**, 5, 162–170.
- [17] L. Frydman, T. Scherf, A. Lupulescu, *Proc. Natl. Acad. Sci. USA* **2002**, 99, 15858–15862.
- [18] a) A. Tal, L. Frydman, *Prog. Nucl. Magn. Reson. Spectrosc.* **2010**, 57, 241–292; b) R. Schmidt, L. Frydman, *Magn. Reson. Med.* **2012**, DOI: 10.1002/mrm.24470.
- [19] S. D. Swanson, *J. Magn. Reson.* **1991**, 95, 615–618.
- [20] M. Kim, J. Gillen, B. A. Landman, J. Zhou, P. C. M. van Zijl, *Magn. Reson. Med.* **2009**, 61, 1441–1450.
- [21] a) M. T. McMahon, A. A. Gilad, J. Y. Zhou, P. Z. Sun, J. W. M. Bulte, P. C. M. van Zijl, *Magn. Reson. Med.* **2006**, 55, 836–847; b) P. Z. Sun, *Magn. Reson. Med.* **2012**, 67, 936–942.
- [22] D. C. Williamson, J. Närväinen, P. L. Hubbard, R. A. Kauppinen, G. A. Morris, *J. Magn. Reson.* **2006**, 183, 203–212.
- [23] a) J.-S. Lee, R. R. Regatte, A. Jerschow, *J. Magn. Reson.* **2012**, 215, 56–63; b) J.-S. Lee, P. Parasoglou, D. Xia, A. Jerschow, R. R. Regatte, *Sci. Rep.* **2013**, 3, 1707.